GCAGS JOURNAL
A Publication of the Gulf Coast Association of Geological Societies
www.gcags.org

Depositional Processes at the Lower Wilcox Shelf–Slope Transition Zone

Mariana I. Olariu and Hongliu Zeng

Bureau of Economic Geology, The University of Texas at Austin, P.O. Box X, Austin, Texas 78758, U.S.A.

ABSTRACT

Recognition of sand bypass at the shelf margin is key to deep-water exploration. This study examines the shelf margin architecture of the Lower Wilcox Group in Texas by combining wireline log with 3D seismic data. During the early Paleocene a relatively extensive (50 km wide), shallow-shelf platform extended across Central Texas making it difficult for the deltas to reach the shelf edge. The seaward pinchout of Lower Wilcox sandstone-rich shoreface deposits is about 20 km updip from the contemporaneous shelf edge indicating that sand remained on the inner and middle shelf and that the shelf margin grew through mud accretion. Highstand sea-level conditions favored the generation of hyperpycnal flows that incised into shelf deposits, with sand bypassed onto upper and middle slopes. In areas of shale withdrawal, extensional features such as growth faults produced long, linear to arcuate strike-elongate depocenters within hanging-walls of faults and dictated sediment delivery pathways. Our work suggests that significant volumes of deep-water sands were deposited from hyperpycnal flows initiated by direct river effluents that accumulated on the upper slope. High-density hyperpycnal flows created sand-filled slope-channel complexes 10–20 m thick and 200 m to more than 1 km wide that served as conduits for bypass to the basin floor. Unconfined, low-density hyperpycnal flows deposited lobes on the upper slope. Lobes spread 10–20 km laterally and 2–4 km downdip, with a maximum total sand thickness of 100 m. A high net-to-gross ratio (0.6) suggests the sand-rich component of the flow was deposited on the upper slope, while finer-grained sediment continued downslope. The shelf-margin architecture exhibited by this sequence serves as an example of hyperpycnal flows being the main initiator of turbidity currents for sand accumulation on the slope.

INTRODUCTION

In the Gulf of Mexico extensive Lower Wilcox deep-water turbidites form a significant exploration target, yet the connection to contemporaneous shallow water reservoirs is poorly documented (Winker, 1982; Galloway et al., 2000; Zarra, 2007; McDonnell et al., 2008). Wilcox shoreline successions (Fisher and McGowen, 1967; Galloway et al., 2000; Olariu and Ambrose, 2016; Zhang et al., 2019; Ambrose et al., 2020; Zhang et al., 2022) and upper-slope deposits (Olariu and Zeng, 2018; Olariu, 2023) have been previously described, and turbidite systems in the deep basin (Meyer et al., 2005) have been drilled, but relatively little is known about the intervening paleoslope.

Because of the scarcity of cores and wireline logs that penetrate deep Lower Wilcox strata, the slope architecture and the dynamics of sediment transport at the shelf break to slope transition zone is not yet well understood (McDonnell et al., 2008). Sand deposition on the continental shelf and across the shelf margin remains understudied, mainly because of the difficulty to explain significant cross-shelf transport of sand, particularly during sea-level highstand (Steel et al., 2018).

Sediment distribution and source-to-sink analysis are best undertaken by integrating 3D seismic with wireline log data to provide a better understanding of the relationship between structures and sedimentation (Moscardelli et al., 2012). This study uses 3D seismic and wireline log data to reveal large-scale upper slope geometries of the Lower Wilcox Group in Central Texas. However, the Lower Wilcox section off the shelf edge is notoriously difficult to interpret using seismic data (Lewis et al., 2007) because of deep burial, complex structure (growth faults and shale ridges), and low data frequency (20 Hz) and resolution (50 m at 4000 m/s). A new workflow that incorporates machine learning with seismic lithology and geomorphology interpretations was tested for quantitative mapping of sandstone thickness and net-to-gross ratio. The procedure is a significant update to current qualitative seismic stratigraphic and seismic attribute approaches for better geologic and reservoir prediction with higher resolution and accuracy.

GEOLOGIC SETTING

The Lower Wilcox Group in Texas has been interpreted as a large-scale, 3rd order clastic wedge of the Rockdale delta system (Fisher and McGowen, 1967; Xue and Galloway, 1993). The

Manuscript received May 30, 2023; revised manuscript received August 7, 2023; manuscript accepted August 7, 2023.

GCAGS Journal, v. 12 (2023), p. 33–44.
https://doi.org/10.62371/EUGP1650

Lower Wilcox sequence (up to 1500 m thick) is bounded by regional flooding surfaces associated with the Big Shale at the top and Midway Shale at the base (Xue and Galloway, 1993; Galloway et al., 2000; Hargis, 2009) and consists of three major intervals (Fig. 1) called A, B and C "deltas" (Fisher and McGowen, 1967; Hargis, 2009).

Lower Wilcox sediments were deposited in seven depocenters (Fig. 2) forming the Rockdale delta system in the Houston Embayment (Fisher and McGowen, 1967). The southernmost Guadalupe deltas (Fig. 2) were recently interpreted as mixed depositional systems (Olariu and Ambrose, 2016; Zhang et al., 2019) based on the variable proportions of fluvial, tide and wave-influenced facies present in cores. This study investigates in detail the shoreline to shelf-to-slope outbuilding of the Lower Wilcox Guadalupe A deltas.

After a major transgression associated with Midway Shale, the earliest deltas of the Lower Wilcox prograded under highstand conditions over a shallow and wide shelf that extended across south-central Texas (Hargis, 2009; Galloway et al., 2000; Crabaugh, 2001; Olariu and Zeng, 2018; Olariu, 2023). The Lower Wilcox deltas were fed by rivers that drained active mountain belts during the humid Greenhouse climate of the late Paleocene, conditions ideal for the generation of hyperpycnal flows (Sweet and Blum, 2011). River-dominated, wave- and tide-influenced deltas on the inner and middle shelf provided sandstone via hyperpycnal flows to the outer shelf (Olariu and Zeng, 2018). These flows eroded the underlying substrate and cut channels into the upper slope.

METHODS

We studied Lower Wilcox strata above Midway shale using a 1000 km^2 3D seismic volume and wireline logs from more than 800 wells. The study area is centered in Gonzales, Dewitt, Karnes and Goliad counties (Fig. 3). Overpressure shale and section expansion due to the presence of growth faults inhibit deeper well penetrations in the most downdip areas. The downdip termination of well control is approximately 10 km south of the Cretaceous shelf margin. Only a few deep (about 6000 m) wells penetrate the entire Lower Wilcox section in the southern part of the study area. Spontaneous potential (SP) log curves were used for subsurface correlation, achieved using the genetic sequence approach of Galloway (1989). Lithologies such as sandstone and shale were interpreted from SP log patterns through log normalization and cutoff values. Normalization was done according to a type of SP curve (with -28 mV for sandstone-shale cutoff). SP values less than -28 mV were used to build sandstone thickness maps. The estimation of sandstone thickness between surfaces of interest was achieved in Petra^{TM} software and entailed the creation of a grid using the least squares method.

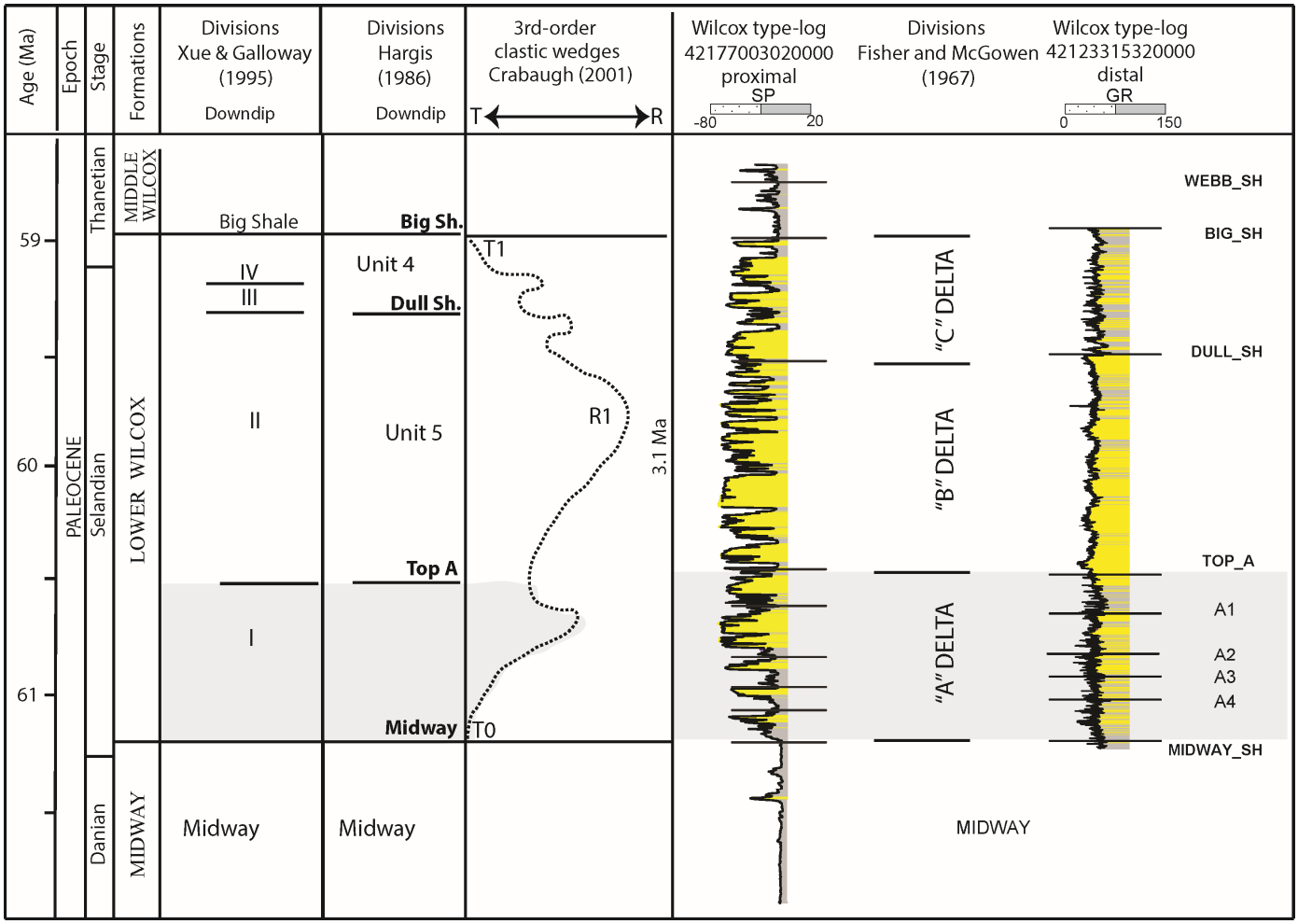

Figure 1. Correlation chart showing lithostratigraphic units for the Lower Wilcox Group in Texas. Depositional environments are interpreted based on sandstone body morphology in the subsurface and provide the basis for subdividing the Wilcox Group into major regressive-transgressive cycles. Proximal (SP) and distal (GR) type well logs show the main stratigraphic subdivisons of the Lower Wilcox Group between the Top A and Midway log markers.

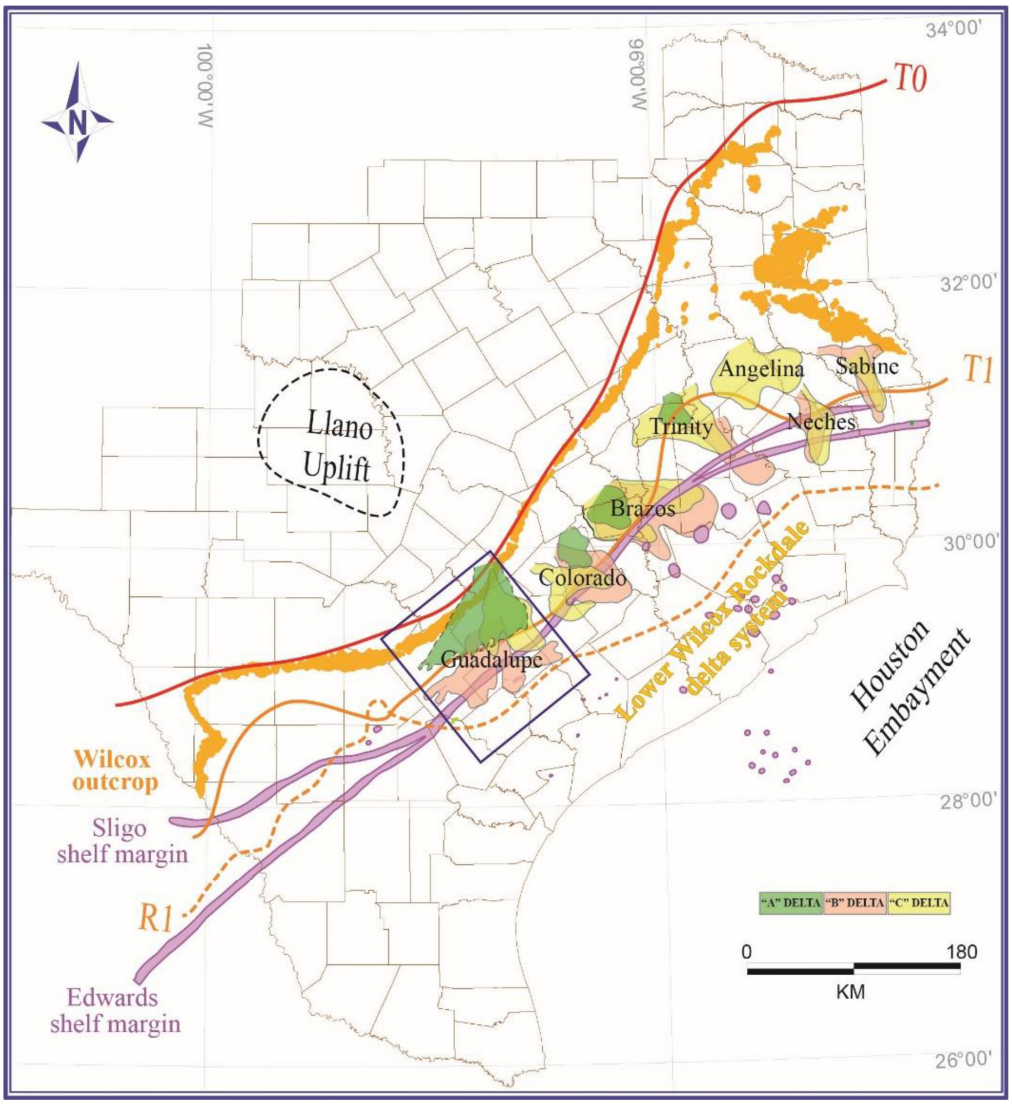

Figure 2. Paleogeographic map depicting paleoshoreline positions in the Lower Wilcox Group (study area—Guadalupe A delta-indicated by blue rectangle). The Lower Wilcox Group was deposited along 7 depocenters in the Rockdale delta system in the Houston Embayment (modified after Fisher and McGowen [1967]). Maximum regressive (R1) and transgressive (T1) shoreline positions (from Crabaugh [2001]) delineate the main clastic wedges. Cretaceous carbonate shelf margins (Sligo and Edwards) and salt domes are shown in purple.

The seismic data set used for this research is a conventional 3D volume with a dominant frequency of 25 Hz. Calculated resolvable limit (a quarter wavelength) is about 20 ms (40 m) at roughly 4000 m/s. Line spacing is 33.5 m at a sample rate of 4 ms. The data are -90° phased for a sense of relative impedance and an optimal tie to wireline logs (SP, gamma ray [GR], and sonic). Although seismic facies and amplitude maps, and seismic inversion are useful to image the general trends they are not able to disclose the presence and extent of the massive sandstone distribution in the intraslope basins in the area. Albeit logs in some wells exhibit exceptionally thick sand deposits, they look similar to less-sandy sediments in seismic amplitude sections. A new machine learning workflow was applied that handily catches nonlinear correlation between lithology logs (e.g., GR) and seismic attributes. This workflow was incorporated with seismic lithology and geomorphology for quantitative mapping of sandstone thickness (for an in-depth description of the method, see Zeng et al. [2021, 2023]). The value of machine learning approach is shown by an improved correlation between wireline log calculated lithology (sand/shale content) and seismic impedance. In addition to excellent fit to training wells, the results expressed good ties to GR and shale volume curves at blind test wells, ensuring a high confidence level for stratigraphic and depositional interpretation.

RESULTS

Structural Deformation

Growth faults were formed on the outer shelf and upper slope during Lower Wilcox deposition and separated minibasins a few km wide and tens of km long. NE–SW trending faults (Fig. 3) provide meter to tens of meter-scale expansion of the stratigraphy (Figs. 4 and 5) and evidence for instability. Accommodation of the growth strata is created by deformation of the underlying slope mudstones, inferred to have had high initial porosities, and thus were easily mobilized (Winker, 1982; Galloway et al., 2000). Along the central Texas Gulf Coast, the Cretaceous Edwards and Sligo reef tracts are stacked (May, 1993). Therefore, Wilcox growth faults sole-out below the Sligo shelf edge (May, 1993) and maintain their position by continual expansion rather than stepping outward (Fig. 5B). The seismic reflection profiles display inclined stratal reflectors displaced by faults in the Lower Wilcox Group. Faults flatten downward from nearly vertical to less than 30°. Significant fault offsets (more than 500 m) and section expansion occur in the Lower Wilcox Group (Fig. 5B). The location of the shelf margin was interpreted from seismic reflection profiles based on an increased gradient at clinoform rollover.

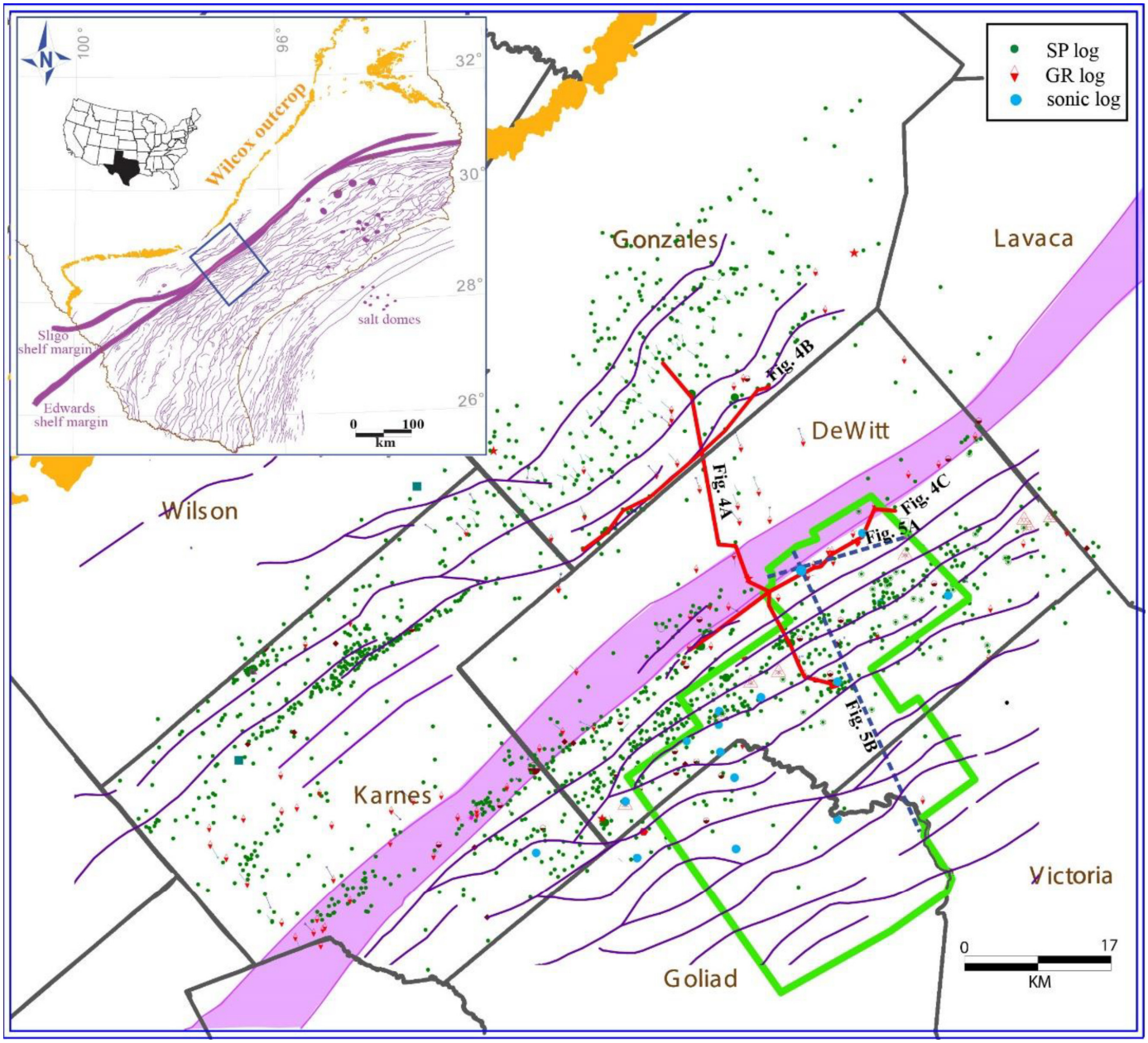

Figure 3. Location map of the study area. Subsurface control consists of wireline logs (mainly SP curves) from about 800 wells. Stratigraphic dip and strike cross-sections (red) and seismic profiles (blue) are shown in Figures 4 and 5, respectively. Location of the 3D seismic dataset is highlighted in green. The inset shows the Cretaceous carbonate shelf margins (Sligo and Edwards) and salt domes in purple (modified from Ewing, 1986). Closely spaced normal faults (purple lines) extend over considerable distances (tens of km) along strike. The structural strike (NE–SW) is parallel to the present-day coastline and to depositional strike.

Shoreline and Shelf Depositional Systems

At the time of commencement of Lower Wilcox progradation the earliest shorelines were located slightly updip of the present-day outcrop belt (Crabaugh, 2001; Hargis, 2009). Deltaic progradation across the shelf concluded with the deposition of 4 parasequences. Sandstone thickness maps show different architectures for the four successive deltaic complexes and net southward movement (Fig. 6). The first progradation advanced the shoreline 30 km basinward; the deltaic sandstones have a maximum thickness of 52 m (average 10 m) (Fig. 6A). The next progradation brought the deltas about 10 km closer to the shelf margin (Fig. 6B); the sandstones reach a maximum thickness of 60 m (average 23 m). There was an 8 km shoreline advance during the next cycle (Fig. 6C); the maximum sandstone thickness is 58 m (average 23 m). The youngest deltaic complex remained in the same position as the previous delta, but supplied more sediment to the shoreline (Fig. 6D); the sandstone thickness reaches a maximum of 68 m (average 24 m). As the Guadalupe A deltas advanced towards the shelf margin the depositional style changed from progradational to aggradational (Olariu, 2023). Sandstone thickness maps show a lobate, dip-elongate geometry for the older deltas (Figs. 6A–6C) indicating fluvial-dominated and tide-influenced conditions, whereas the younger deltas display a more strike-elongate configuration suggesting more wave reworking (Fig. 6D). As the deltas did not reach the shelf edge the outer shelf was mud-dominated.

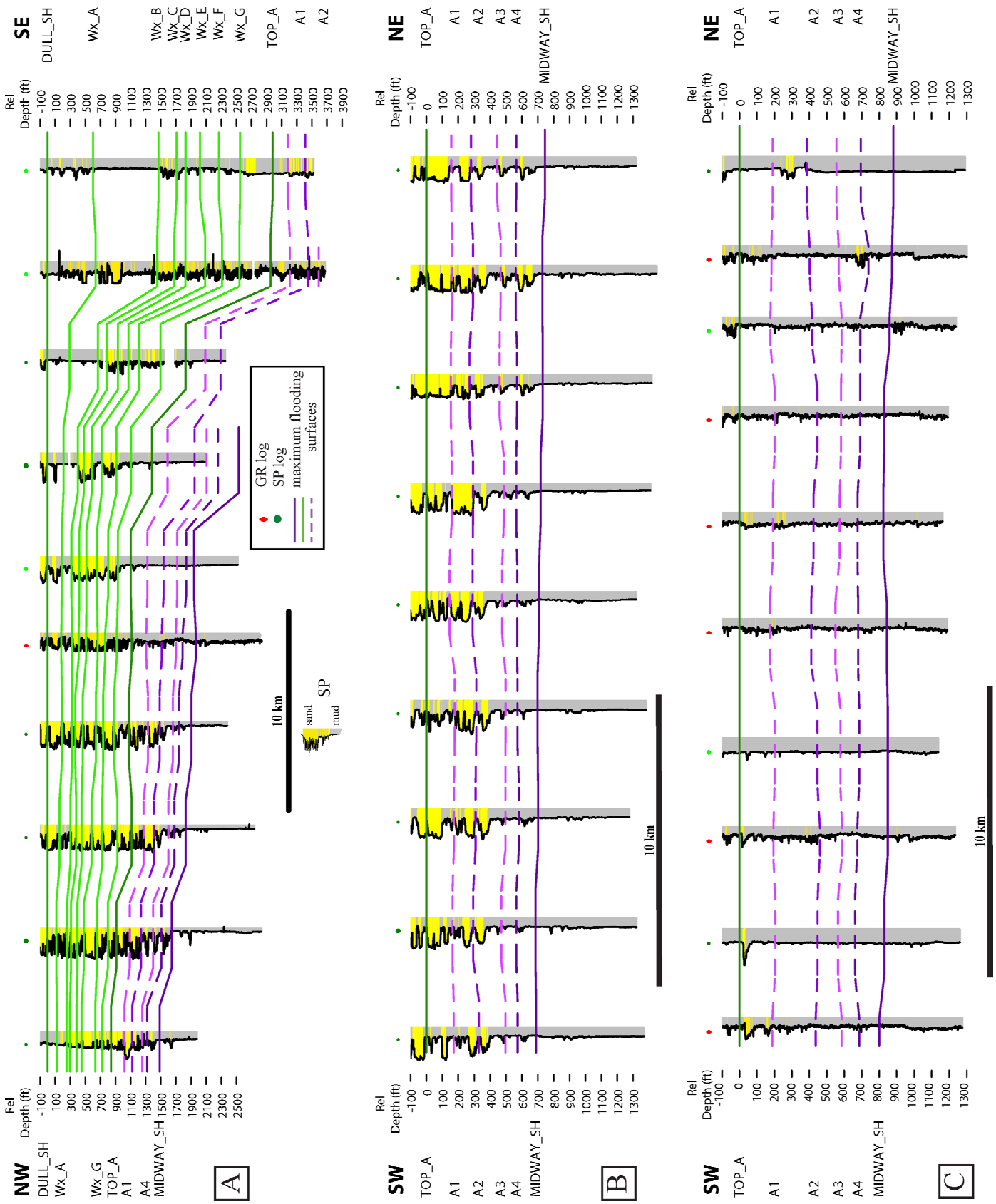

Figure 4. Stratigraphic cross-sections through the Lower Wilcox Group. Spontaneous potential (SP) curves are used for correlation. The stratigraphy and thickness trends of the Wilcox Group are affected by normal faults. Maximum flooding surfaces (green, purple) separate 4th order cycles (for location see Figure 3). (A) Stratigraphic dip section (datum Dull shale). (B) Stratigraphic strike section in proximal setting, inner to middle shelf (datum Top A). (C) Stratigraphic strike section in distal setting, outer shelf (datum Top A).

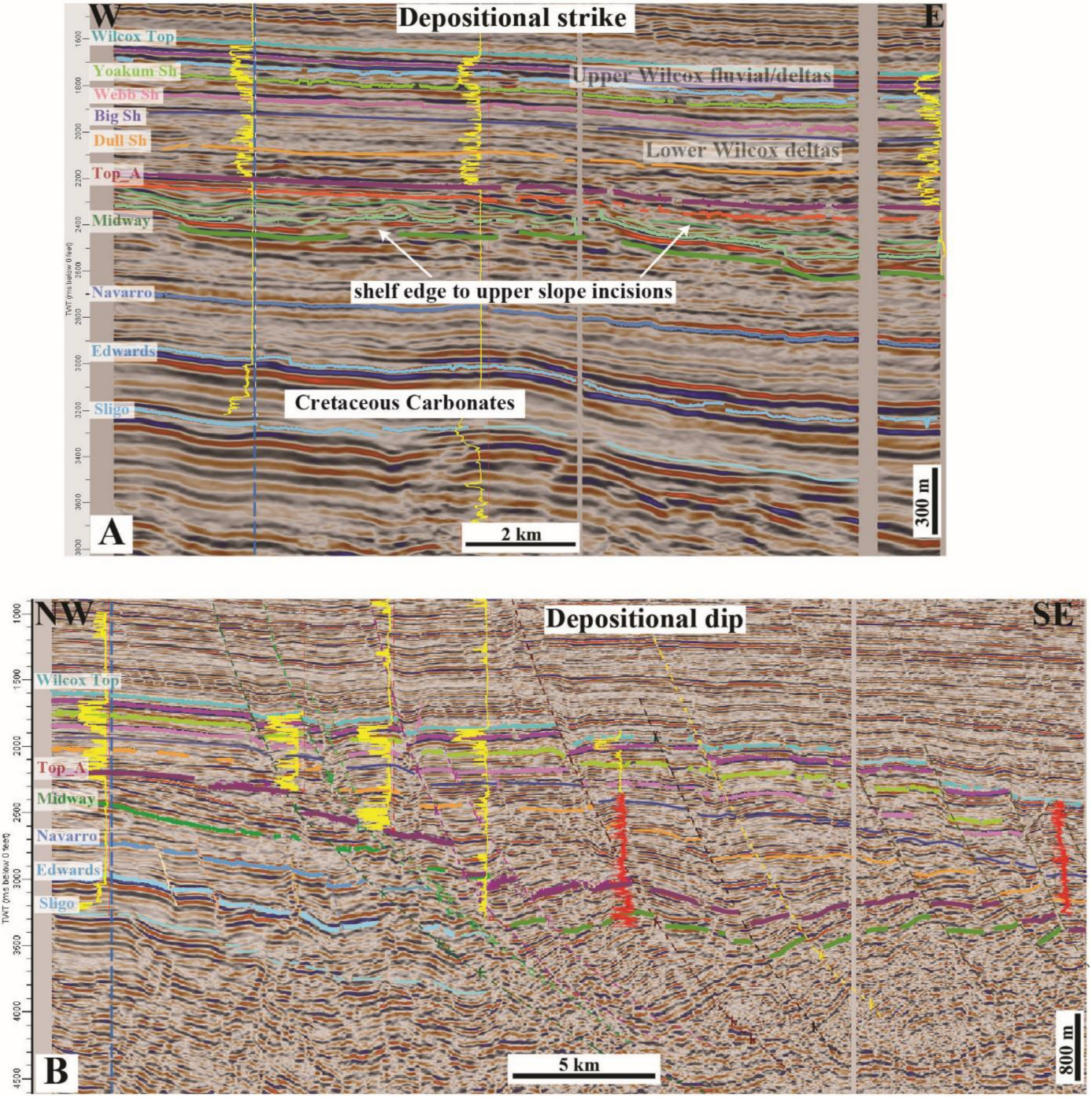

Figure 5. Seismic profiles illustrate the interaction between Lower Wilcox stratigraphy and faults (see Figure 3 for location). (A) Oblique-strike (W–E) oriented seismic section. Shelf edge and upper slope incisions are present in the Lower Wilcox Delta A interval. (B) Oblique-dip (NW–SE) oriented seismic section. All faults exhibit syn-sedimentary growth, with thickened sedimentary units on downthrown sides. Major faults have basinward dips toward the southeast that decrease with depth from nearly vertical to less than 30°. Offsets become progressively less upsection, suggesting that rates of fault movement decreased over time.

Slope Architecture and Depositional Evolution

Lower Wilcox upper slope depositional systems are identified in seismic-derived sandstone thickness maps (Fig. 7) and verified by crosschecking with seismic profiles and wells. Wireline logs constrain lithologic interpretations, and in conjuncture with the 3D seismic data, provide a robust interpretation of the upper slope architecture. There are substantial sandstone accumulations (high average thickness to width) in intraslope minibasins formed by growth fault development (Fig. 7). On seismic-derived sandstone thickness maps, individual channels are difficult to resolve, except in the updip area close to the shelf edge where maps show a mixture of both vertical and lateral stacking of dip-elongate (NW–SE) geometries (Fig. 7). Based on the location in the proximity of the shelf edge rollover (Fig. 5B) and the overall sandy fill, as suggested by higher seismic reflectivity (Fig. 7) these channels are interpreted as shelf edge to upper slope gullies. Channels were initiated in the upper part of the slope as rela-

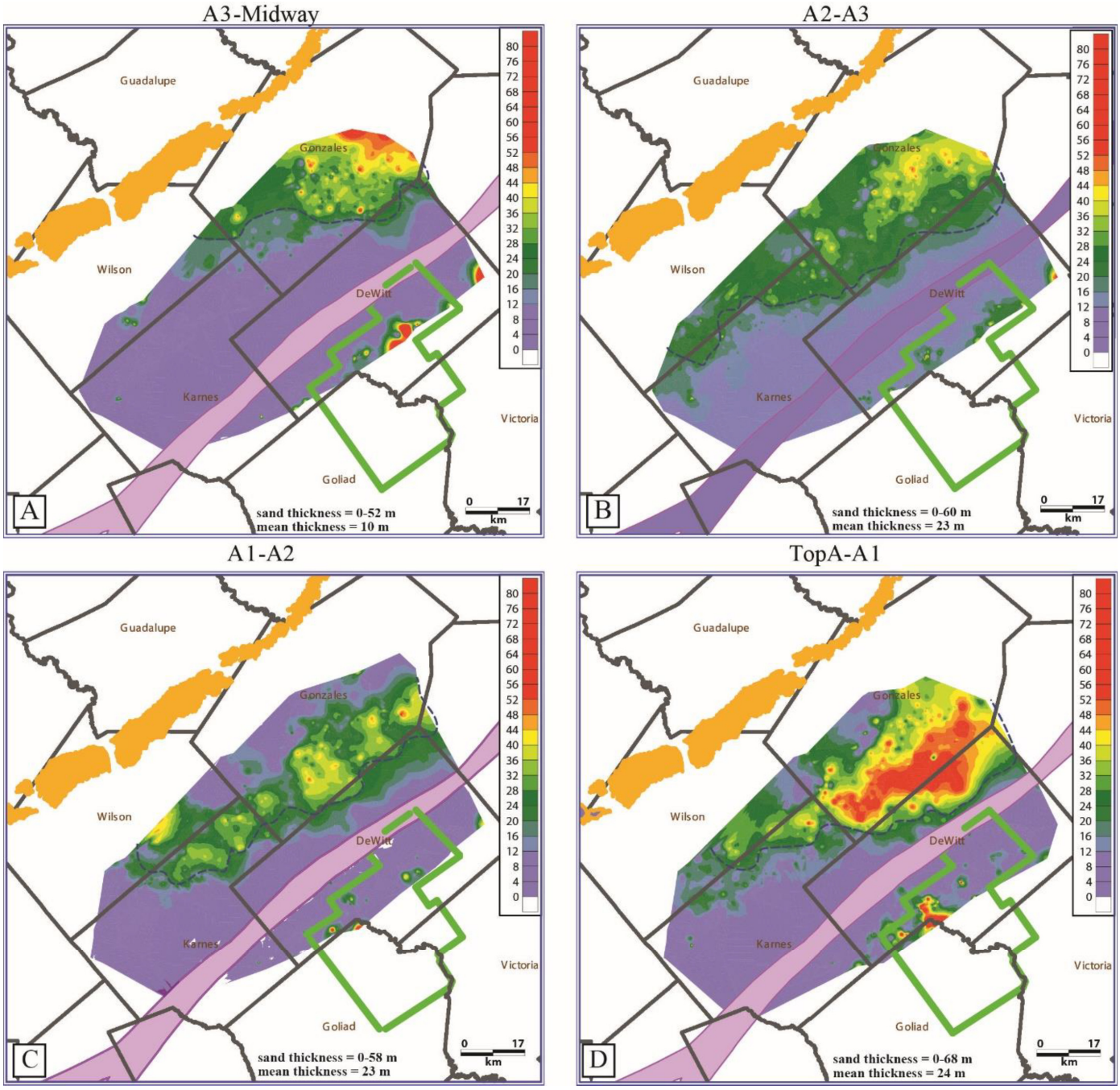

Figure 6. Sandstone thickness maps (obtained from wireline logs) for the 4th order cycles of the Lower Wilcox Guadalupe A Delta. Deltaic shorelines depicted in A (oldest) to D (youngest) are: (A) between Midway Shale and A3; (B) between A3 and A2; (C) between A2 and A1; and (D) between A1 and Top A. Shoreline positions are indicated by a white dashed line in each map. The maximum sandstone thickness of individual deltaic complexes in the cycles ranges from 52 m to 68 m. Dip-elongate (NE–SW) sandstone morphologies suggest river dominance in the older cycles; the youngest one shows a strike-elongated pattern indicating more wave influence. Stratigraphic nomenclature in the Lower Wilcox Group is shown in wireline log cross sections in Figure 4.

tively small (100–200 m wide) linear features (Fig. 5A). Stacked channel sandstone thickness ranges from 10 to 50 m. Sandstone-filled channel complexes range in size from 200 m to more than 1 km wide and 100 m thick (Fig. 7). Unconfined, sheet-like deposits formed lobes down slope. Lobes spread 10-20 km laterally and 2–4 km downdip with a maximum total net sandstone thickness of 100 m and maximum net-gross ratio of 0.6 (Fig. 7). At seismic resolution, a high-frequency cycle encompasses about 200 m sediments in average. In depocenters, accumulated sand thickness in multiple high-frequency units is as high as 500 m.

Sediment Volumes in Compartments and Trends through Time

Relative sediment storage for each cycle, as well as volumes of sandstone and shale for both the topset (shoreline and shelf) and upper slope compartments were estimated (Fig. 8). The trend in total volume is well-correlated with trend in shale volume, but

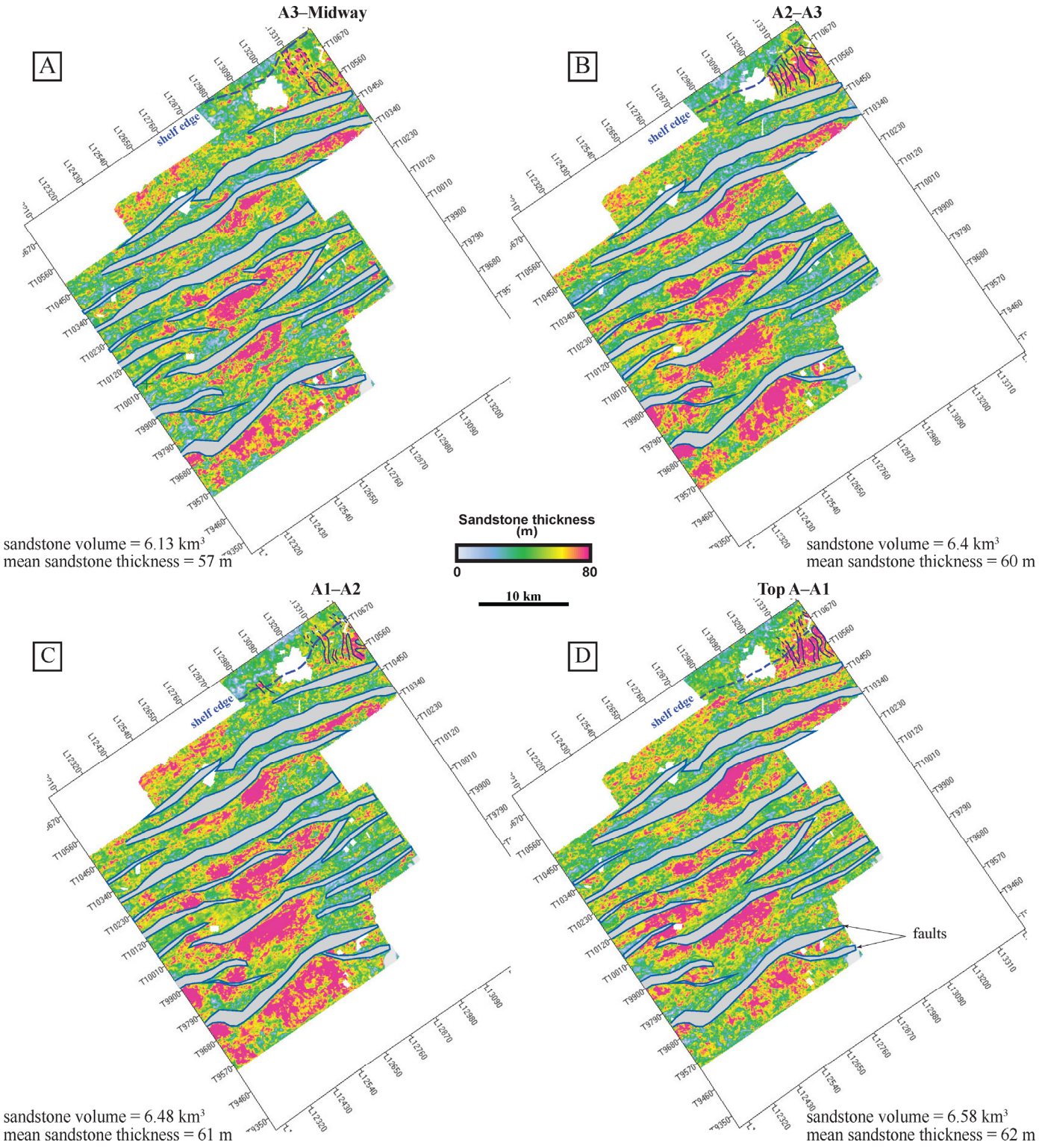

Figure 7. Sandstone thickness maps (obtained from 3D seismic interpretations) show Lower Wilcox significant sand accumulations in intraslope minibasins formed by growth faults (light gray). Slope depocenters depicted in A (oldest) to D (youngest) are: (A) between Midway Shale and A3; (B) between A3 and A2; (C) between A2 and A1; and (D) between A1 and Top A. At seismic resolution, a high-frequency cycle accumulates about 200 m sediments in average. Sandstone-filled upper slope channel complexes (blue lines) range in width from 200 m to more than 1 km. Lobes spread 10–20 km laterally and 2–4 km downdip, with a maximum total sand thickness of 100 m. In depocenters, accumulated sand thickness in multiple high-frequency units is as high as 500 m. Higher seismic reflectivities (bright amplitudes) were interpreted as sandstone, whereas lower reflectivities (darker colors) as shale. Stratigraphic nomenclature in the Lower Wilcox Group is shown in wireline log cross sections in Figure 4.

only a minor correlation exists with sandstone volumes. Although volume of shale comprises the bulk of sediment in each cycle, the sandstone volume increases (51 to 95 km^3) with time and net-to-gross ratio (0.16 to 0.32) as well for the topset compartment (Fig. 8). The calculated areas are slightly different because our results are sensitive to the number of available wireline logs (limited by penetration depth) for each cycle. The estimated upper slope accumulated sandstone volumes become greater with time (6.13 to 6.58 km^3), as well as sandstone thickness (57 m to 62 m), albeit the differences are small between cycles (Figs. 7 and 8). However, the upper slope net-to-gross ratio slightly decreases with time (0.64 to 0.61).

DISCUSSION

The shelf-margin architecture depicted by the Guadalupe Lower Wilcox A sequence is an example of a deep-water system in which hyperpycnal flows are the main initiators of turbidity currents for sand accumulation on the upper slope. Hyperpycnal flows are river-derived gravity currents capable of transporting considerable volumes of sediment from the shoreline onto the shelf and slope (Piper and Normark, 2001; Mellere et al., 2002; Mulder et al., 2003; Plink-Björklund and Steel, 2004; Soyinka, and Slatt, 2008; Steel et al., 2008; Olariu et al., 2010; Steel at al., 2018). However, sand deposition on the outer shelf remains under-studied, mainly because few mechanisms explain substantial cross-shelf transport of sand, especially during sea-level highstand (Steel et al., 2018). Processes commonly thought to transport sediment on continental shelves include tide and waves, but gravity-driven processes may also play an important role in sediment transfer from river to deeper water (Petter and Steel, 2006; Gan et al., 2022), especially when the deltas do not reach the shelf margin. River-dominated, wave- and tide-influenced Guadalupe A deltas on the inner and mid shelf provided sandstone via hyperpycnal flows to the outer shelf and upper slopes (Olariu and Zeng, 2018). After Midway transgression, earliest Lower Wilcox deltas prograded during highstand conditions over a shallow and relatively wide shelf (Olariu and Ambrose, 2016) during the humid Greenhouse climate of the late Paleocene (Sweet and Blum, 2011), ideal conditions for the initiation of hyperpycnal flows. Increased sediment influx during Late Paleocene was controlled by periodic climate warming during hyperthermals and concurrent active uplift (Carvajal et al., 2009). Exceptional flood episodes are thought to have been common during Lower Wilcox time and help explain the presence of hyperpycnites on the outer shelf (Olariu and Zeng, 2018). Hyperpycnal activity (frequency and magnitude) increases if relative sea level rises in an area with a wide shelf (Mulder and Alexander, 2001). In this case, river-sediment discharge directly bypasses the shelf-edge and generates turbidity currents that feed sediment to the deep-water areas (Plink-Björklund et al., 2001; Mellere et al., 2002). In the Lower Wilcox Guadalupe A deltas, hyperpycnal flows had erosive potential that allowed them to erode the underlying substrate and cut channels into the upper slope (Fig.7). Where a canyon head is not directly linked to the river, or the delta is not at the shelf edge, river-generated hyperpycnal flows are most commonly the major connector of sediment from river to the shelf–slope transition zone (Plink-Bjorklund and Steel, 2004; Gamberi et al., 2020; Gauchery et al., 2021). Since hyperpycnal flows are essentially sediment-gravity currents, flooding events provide more sediment and more discharge (Mulder and Syvitski, 1995; Gan et al., 2022).

Episodic, high-density hyperpycnal flows are held responsible for cross shelf transport of sediment during the Lower Wilcox time (Olariu and Zeng, 2018). These flows bypassed the clinoform rollover, incised into shelf deposits, and delivered sand to the upper slopes (Fig. 7). Irregular flows are thought to have higher flux rates, being able to transport more sediment into distal slope settings than lower-flux-rate sustained flows of longer duration (Cosgrove et al. 2020). Therefore, there is a continuous transition from shelf to slope with abundant hyperpycnal deposits in the associated outer shelf and upper slope channels, as well as a lower proportion of slumped strata, denoting the continuity of the fluvial influence on the system (Cosgrove et al. 2020). Relatively small (200 m to 1 km wide; 50 to 100 m deep) sandstone-filled channel complexes cut into Guadalupe A muddy shelf (Fig. 7). Hyperpycnites in upper slope channels can be recognized by the connection of the channels updip with fluvial channels (Petter and Steel, 2006; Gomis-Cartesio et al., 2016). The lack of wireline logs and limited extent of the seismic data set (Fig. 3) made it hard to see the connections of the slope incisions at the shelf edge with the distributary channels on the Lower Wilcox shelf. However, there is evidence from core (Olariu and Zeng, 2018; Olariu, 2023) that implies hyperpycnal processes at the shelf-slope transition zone. The absence of seismic-scale slumps and large canyons (Fig. 7) also suggests that the slope system was fed by another mechanism than over steepening and collapse of the shelf edge or upper slope reaches.

By contrast, incisions such as, Lavaca canyon and Hallettsville complex, located laterally along depositional strike, cut into the outer shelf and shelf margin of Lower Wilcox Colorado A delta system, but they are filled mostly with mud and sparse sandstone beds interpreted as submarine channel and debris-flow deposits (McDonnell et al., 2008; Clayton and Olariu, 2022). These incisions have significant depths (hundred to thousands of meters) and carve into the shelf for considerable (tens of km) distances (Clayton and Olariu, 2022; Fisher et al., 2021). Lavaca canyon (3.2 km long and 1.6 km wide) cuts downward through almost all the Lower Wilcox Colorado A delta (Chuber, 1979). Progradation of the Colorado A deltas repeatedly advanced to the shelf edge and instability increased as successive deltaic lobes loaded the margin resulting in failure and re-adjustment of local slope gradients (Galloway and McGilver, 1995), creating large submarine canyons (Berg, 1979; Edwards, 1986).

Lower Wilcox growth faults provide tens of meter scale expansion of stratigraphy (Fig. 4) and evidence for upper slope instability. In areas of shale withdrawal, growth faults produce long strike-elongate depocenters within the hanging-walls and control sediment delivery pathways (Prather, 2003). In the Lower Wilcox Guadalupe A succession, evidence of syn-sedimentary faulting comes from intraslope ponding of flows with laterally amalgamated channels and lobate sand sheets (Fig. 7). Alternation between slope channel and lobe deposition is caused by variability in the magnitude of hyperpycnal activity (Petter and Steel, 2006). Sand was delivered to the upper slope during river floods which provided a large sediment volume that allowed for slope accretion (Olariu and Zeng, 2018). Successive hyperpycnal flows would have avoided the topography created by prior slope-lobe deposits, resulting in progradation of lobes (Prather, 2003). Lower Wilcox upper slope lobes spread 10–20 km laterally and 2–4 km downdip with a maximum total sand thickness of 100 m. Unfortunately, the internal geometry and architecture remain unknown due to the limitation of the seismic resolution and lack of core penetrations. However, a high net-to-gross ratio (0.6) indicates the sand rich component of the flow was deposited on the upper slope while finer grained sediment continued down slope.

The earliest Lower Wilcox deltas crossed only partially the drowned Cretaceous platform despite constantly growing sediment supply because of high accommodation available at the commencement of Wilcox deposition (Olariu, 2023). The shoreline succession exhibits progradational followed by aggradational stacking of Lower Wilcox deltaic cycles (Fig. 6). During sea-level highstand, sediment was supplied to aggrading delta topsets, feeding the growth of successive deltaic lobes and therefore more sediment was trapped on the shelf (Fig. 6) and less deposition occurred on the upper slope with time (Fig. 7). This is also indicated by the upper slope net-to-gross ratio which decreases in

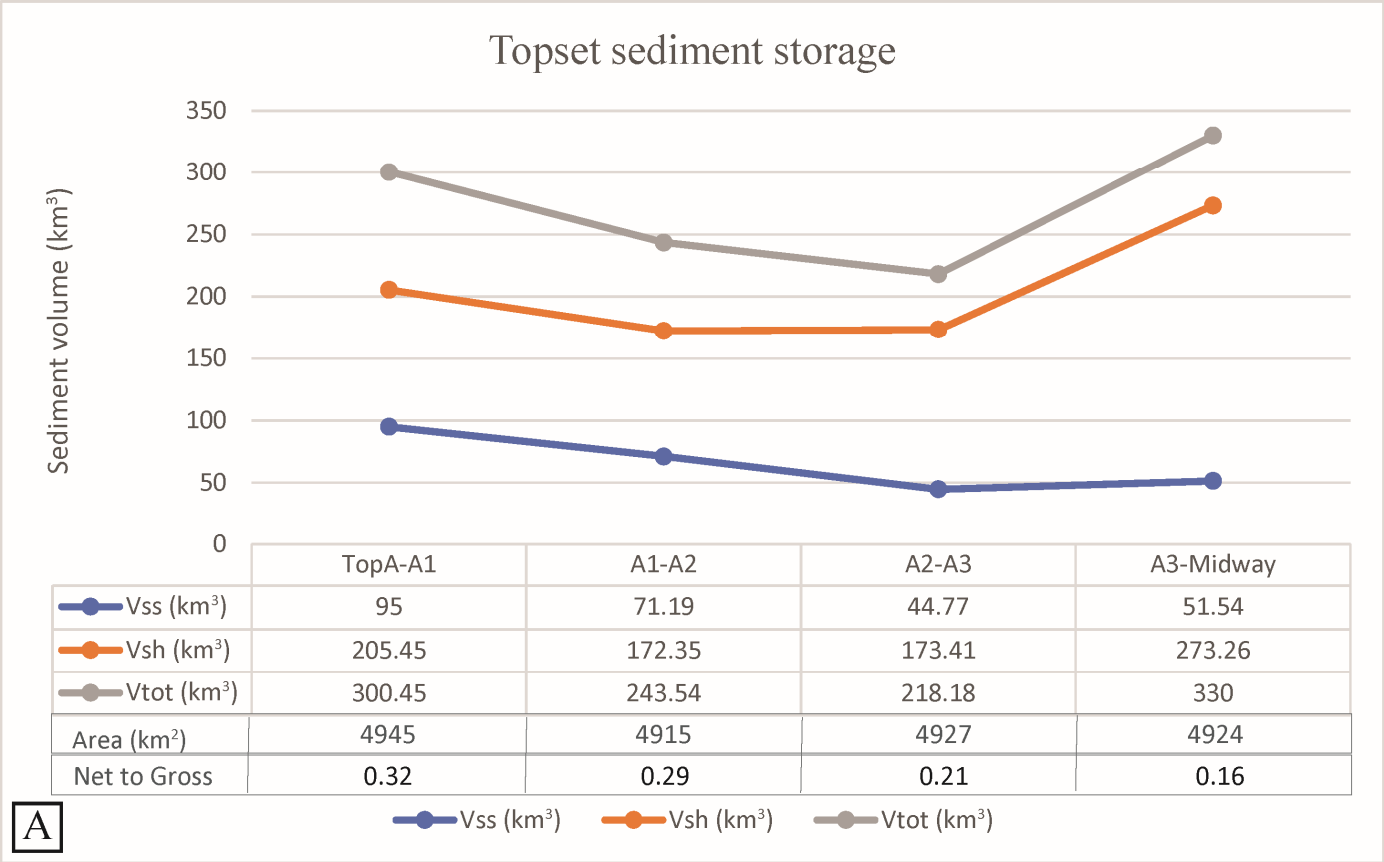

	TopA-A1	A1-A2	A2-A3	A3-Midway
Vss (km³)	95	71.19	44.77	51.54
Vsh (km³)	205.45	172.35	173.41	273.26
Vtot (km³)	300.45	243.54	218.18	330
Area (km²)	4945	4915	4927	4924
Net to Gross	0.32	0.29	0.21	0.16

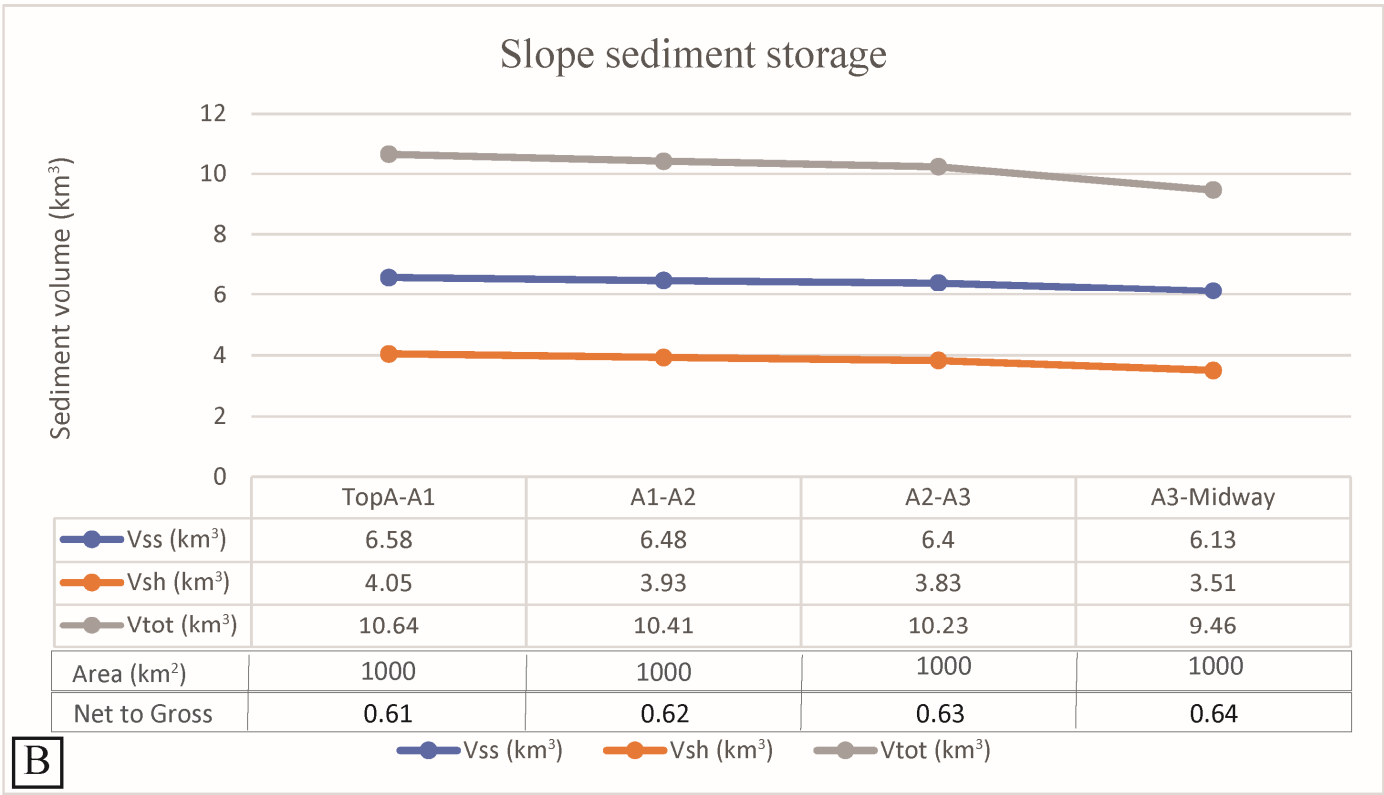

	TopA-A1	A1-A2	A2-A3	A3-Midway
Vss (km³)	6.58	6.48	6.4	6.13
Vsh (km³)	4.05	3.93	3.83	3.51
Vtot (km³)	10.64	10.41	10.23	9.46
Area (km²)	1000	1000	1000	1000
Net to Gross	0.61	0.62	0.63	0.64

Figure 8. Relative sediment storage for each 4th order cycle of the Lower Wilcox Guadalupe A Delta. (A) Topset (shoreline and shelf) sediment storage and (B) upper slope sediment storage, as well as estimated volumes of sandstone and shale for each cycle. Stratigraphic nomenclature in the Lower Wilcox Group is shown in wireline log cross sections in Figure 4.

younger cycles (Fig. 8). There are uncertainties when estimating the shelf to slope Lower Wilcox sediment budgets and partitioning of the shelf margin sedimentary prism because of limited data availability in the middle and lower slope. Systematic stacking patterns of slope architecture are difficult to observe when parts of the slope are observed in isolation (Petter and Steel, 2006).

However, there was bypass and sediment delivery at the shelf edge (Fig. 7) helped by hyperpycnal flows fed directly from rivers during floods (Olariu and Zeng, 2018). A supply-dominated margin during greenhouse time has potential for sand bypass during sea level rise (Carvajal et al., 2009). The flows may even accrete the entire slope and there is evidence of Lower Wilcox sandstone-filled channels in a mid to lower slope position (McDonnell et al., 2008) 90 km downdip from our study area. Bypass of sediment down the slope is also indicated by the presence of large deep-water accumulations (Meyer et al., 2005; Zarra, 2007) during this time.

CONCLUSION

Our work suggests that significant volumes of deep-water sands were deposited from hyperpycnal flows initiated by direct river effluents and accumulated on the upper slope. Continued southwestward progradation across the 50 km wide shelf advanced the shoreline, but the Lower Wilcox Guadalupe A deltas did not reach the shelf edge. The sandstone dominated deltas remained 10–20 km updip from the shelf edge and the shelf margin has grown through the accretion of muddy clinothems. The presence of outer-shelf to shelf-edge incisions had been triggered and sustained by hyperpycnal flows. High-density hyperpycnal flows created sand-filled upper slope-channel complexes 50–100 m thick and 200 m to more than 1 km wide that served as conduits for bypass to the basin floor. Unconfined, low-density hyperpycnal flows deposited lobes on the slope. Lobes spread 10–20 km laterally and 2–4 km downdip, with a maximum total sand thickness of 100 m. A high net-to-gross (0.6) results suggests the sand-rich component of the flow was deposited on the upper slope while finer grained sediment continued down the slope.

ACKNOWLEDGMENTS

The State of Texas Advanced Resource Recovery (STARR) program supported this research. Excellong Inc. provided well and seismic data. The prompt response of the Core Research Center team (Nathan Ivicic and Brandon Williamson) at the Bureau of Economic Geology is greatly appreciated. The author would like to thank William Ambrose, William Fisher and Philomena Gan for their critical reading and comments. Publication authorized by the director of Bureau of Economic Geology, University of Texas at Austin.

REFERENCES CITED

Ambrose, W. A., P. P. Flaig, J. Zhang, M. I. Olariu, C. Denison, T. Demchuk, and J. O'Keefe, 2020, The Midway to Carrizo succession in the southeastern Texas Gulf Coast: Evolution of a tidally-influenced coastline: Gulf Coast Association of Geological Societies Journal, v. 9, p.41–75.

Berg, R. R., 1979, Characteristics of Lower Wilcox reservoirs, Valentine and South Hallettsville fields, Lavaca County, Texas, Gulf Coast Association of Geological Societies Transactions, v. 29, p. 11–23.

Carvajal, C., R. Steel, and A. Petter 2009, Sediment supply: the main driver of shelf-margin growth: Earth-Science Reviews, v. 96, p. 221–248.

Chuber, S., 1979, Exploration methods of discovery and development of Lower Wilcox reservoirs in Valentine and Menking fields, Lavaca County, Texas: Gulf Coast Association of Geological Societies Transactions, v. 29, p. 42–51.

Clayton, C. A., and C. Olariu, 2022, Tectonic preconditioning of recurrent largescale canyon incisions; example from Cretaceous and Paleogene of northern Gulf of Mexico, Marine Geology, v. 453, p. 1–14.

Cosgrove, G. I. E., M. Poyatos-Moré, D. R. Lee, D. M. Hodgson, W. D. McCaffrey, and N. P. Mountney, 2020, Intra-clinothem variability in sedimentary texture and process regime recorded down slope profiles: Sedimentology, v. 67, p. 431–456.

Crabaugh, J. F., 2001, Nature and growth of nonmarine-to-marine clastic wedges: Examples from the Upper Cretaceous Iles Formation, Western Interior Basin (Colorado) and the Lower Paleogene Wilcox Group of the Gulf of Mexico Basin (Texas): Ph.D. Dissertation, University of Wyoming, 272 p.

Edwards, M. B., 1986, A reappraisal of depositional environment (barrier bar or submarine fan) for Lower Wilcox reservoirs of Valentine field, Lavaca County, Texas Gulf Coast: South Texas Geological Society, p. 252–259.

Ewing, T. E., 1986, Structural styles of the Wilcox and Frio growth-fault trends in Texas: Constraints on geopressured reservoirs, Bureau of Economic Geology Report of Investigations 154, 86 p.

Fisher, W. L., and J. H. McGowen, 1967, Depositional systems in the Wilcox Group of Texas and their relationship to occurrence of oil and gas: Gulf Coast Association of Geological Societies Transactions, v. 17, p. 105–125.

Fisher, W. L., W. E. Galloway, R. J. Steel, C. Olariu, C. Kerans, and D. Mohrig, 2021, Deep-water depositional systems supplied by shelf-incising submarine canyons: Recognition and significance in the geologic record: Earth-Science Reviews, v. 214, p. 1–62.

Galloway, W. E., 1989, Genetic Stratigraphic sequences in basin analysis II: Application to northwest Gulf of Mexico Cenozoic basin: American Association of Petroleum Geologists Bulletin 73 (2), p. 143–154.

Galloway, W. E., and T. A. McGilvery, 1995, Facies of a submarine canyon fill reservoir complex, lower Wilcox Group (Paleocene), Central Texas coastal plain: Turbidites and associated deep-water facies: SEPM (Society for Sedimentary Geology) Core Workshop No. 20, p. 1–24.

Galloway, W. E., P. E. Ganey-Curry, X. Li, and R. T. Buffler, 2000, Cenozoic depositional history of the Gulf of Mexico Basin, American Association of Petroleum Geologists Bulletin 84, p. 1743–1774.

Gamberi, F., C. Pellegrini, G. Dallavalle, D. Scarponi, K. Bohacs, and F. Trincardi, 2020, Compound and hybrid clinothems of the last lowstand mid-Adriatic deep: processes, depositional environments, controls and implications for stratigraphic analysis of prograding systems: Basin Research, v. 32, p. 363–377.

Gan, Y., F. N. De Almeida, V. M. Rossi, R. J. Steel, and C. Olariu, 2022, Sediment transfer from shelf to deepwatwer slope: How does it happen?: Journal of Sedimentary Research, v. 92, p. 570–590.

Gauchery, T., M. Rovere, C. Pellegrini, A. Asioli, T. Tesi, A. Cattaneo, and F. Trincardi, 2021, Post–LGM multi-proxy sedimentary record of bottom-current variability and downslope sedimentary processes in a contourite drift of the Gela Basin (Strait of Sicily): Marine Geology, v. 439, p. 1–24.

Gomis-Cartesio, L. E., M. Poyatos-More, S. S. Flint, D. M. Hodgson, R. L. Brunt, and H. D. V. Wickens, 2016, Anatomy of a mixed-influence shelf edge delta, Karoo Basin, South Africa, Geological Society (London) Special Publications, v. 444, p. 393–418.

Hargis, R. N., 2009, Major transgressive shales of the Wilcox, northern portion of South Texas: South Texas Geological Society Bulletin, v. 49, p. 19–47.

Lewis, J., S. Clinch, D. Meyer, M. Richards, C. Skirius, R. Stokes, L. Zarra, 2007, Exploration and appraisal challenges in the Gulf of Mexico deep-water Wilcox: Part 1—Exploration overview, reservoir quality, and seismic imaging, *in* L. Kennan, J. Pindell, and N. C. Rosen, eds., The Paleogene of the Gulf of Mexico and Caribbean basins: Processes, events and petroleum systems: Proceedings of the 27th Annual Gulf Coast Section of the Society of Economic Paleontologists and Mineralogists Foundation Bob F. Perkins Research Conference, p. 398–414.

May, J. A., 1993, Shelf sandstone of the deep Wilcox trend, central Texas Gulf Coast, *in* E. G. Rhodes and T. F. Moslow, eds., Marine clastic reservoirs: Examples and analogues: Springer-Verlag, p. 135–159.

McDonnell, A., R. G. Loucks, and W. E. Galloway, 2008, Paleocene to Eocene deep-water slope canyons, western Gulf of Mexico: Further insights for the provenance of deep-water offshore Wilcox Group plays: American Association of Petroleum Geologists Bulletin, v. 92, p. 1169–1189.

Mellere, D., P. Plink-Björklund, and R. Steel, 2002, Anatomy of shelf deltas at the edge of a prograding Eocene shelf margin: Sedimentology, v. 49, p. 1181–1206.

Meyer, D., L. Zarra, D. Rains, B. Meltz, and T. Hall, 2005, Emergence of the Lower Tertiary Wilcox trend in the deepwater Gulf of Mexico: American Association of Petroleum Geologists Search and Discovery Article 10084, 11 p., <https://www.searchanddiscovery.com/pdfz/documents/2005/meyer/images/meyer.pdf.html>.

Moscardelli, L., L. J. Wood, and D. B. Dunlap, 2012, Shelf-edge deltas along structurally complex margins: A case study from eastern offshore Trinidad: American Association of Petroleum Geologists Bulletin, v. 96, p. 1483–1522.

Mulder T., J. Syvitski, S. Migeon, J. C. Faugeres, and B. Savoye 2003, Marine hyperpycnal flows: initiation, behavior and related deposits. A review: Marine and Petroleum Geology, v. 20, p. 861–882.

Mulder, T., and J. P. M. Syvitski, 1995, Turbidity currents generated at river mouths during exceptional discharges to the world's oceans: Journal of Geology, v. 103, p. 285–299.

Mulder, T., and R. J. Alexander, 2001, The physical characteristics of sub-aqueous sedimentary density flows and their deposits: Sedimentology, v. 48, p. 269–299.

Olariu, C., R. J. Steel, A. L. and Petter, 2010, Delta-front hyperpycnal bed geometry and implications for reservoir modeling: Cretaceous Panther Tongue delta, Book Cliffs, Utah: American Association of Petroleum Geologists Bulletin, v. 94, p. 819–845.

Olariu, M. I., and W. A. Ambrose, 2016, Process regime variability across growth faults in the Paleogene Lower Wilcox Guadalupe delta, South Texas Gulf Coast: Sedimentary Geology, v. 341, p. 27–49.

Olariu, M. I., and H. Zeng, 2018, Prograding muddy shelves in the Paleogene Wilcox deltas, South Texas Gulf Coast: Marine and Petroleum Geology, v. 91, p. 71–88.

Olariu, M. I., 2023, Sedimentology and stratigraphy of the earliest deltaic shorelines of the Paleocene Lower Wilcox Group in the Gulf of Mexico: Journal of Sedimentary Research, v. 93, p. 522–540.

Petter, A. L., and R. J. Steel, 2006, Hyperpycnal flow variability and slope organization on an Eocene shelf margin, central basin, Spitsbergen: American Association of Petroleum Geologists Bulletin, v. 90, p. 1451–1472.

Piper, D. J. W., and W. R. Normark, 2001, Sandy fans: From Amazon to Hueneme and beyond: American Association of Petroleum Geologists Bulletin, v. 85, 1407–1438.

Plink-Björklund, P., D. Mellere, and R. J. Steel, 2001, Turbidite variability and architecture of sand-prone, deepwater slopes: Eocene clinoforms of the Central Basin, Spitsbergen: Journal of Sedimentary Research, v. 71, p. 897–914.

Plink-Björklund, P., and R. J. Steel, 2004, initiation of turbidity currents: outcrop evidence for Eocene hyperpycnal flow turbidite: Sedimentary Geology, v. 165, p. 29–52.

Prather, B. E., 2003, Controls on reservoir distribution, architecture and stratigraphic trapping in slope settings: Marine and Petroleum Geology, v. 20, p. 529–545.

Soyinka, O., and R. M. Slatt, 2008, Identification and microstratigraphy of hyperpycnites and turbidites in Cretaceous Lewis Shale, Wyoming: Sedimentology, v. 55, p. 1117–1133.

Steel, R., C. Carvajal, A. Petter, C. Uroza, et al., 2008, Shelf and shelf-margin growth in scenarios of rising and falling sea level, *in* G. Hampson, R. Steel, P. M. Burgess, and R. W. Dalrymple, eds., Recent advances in models of siliciclastic shallow-marine stratigraphy: Society of Economic Paleontologists and Mineralogists Special Publication 90, p. 47–71.

Steel, E., A. R. Simms, R. Steel, and C. Olariu, 2018, Hyperpycnal delivery of sand to the continental shelf: Insights from the Jurassic Lajas Formation, Neuquen Basin, Argentina: Sedimentology, v. 65, p. 2149–2170.

Sweet, M. L., and M. D. Blum, 2011, Paleocene-Eocene Wilcox submarine canyons and thick deepwater sands of the Gulf of Mexico: Very large systems in a greenhouse world, not a Messinian-like crisis: Gulf Coast Association of Geological Societies Transactions, v. 61, p. 443–450.

Winker, C. D., 1982, Cenozoic shelf margins, northwestern Gulf of Mexico Basin: Gulf Coast Association of Geological Societies Transactions 32, p. 427–448.

Xue, L. and W. E. Galloway, 1993, Sequence stratigraphic and depositional framework of the Paleocene Lower Wilcox strata, northwest Gulf of Mexico Basin: Gulf Coast Association of Geological Societies Transactions, v. 43, p. 453–464.

Zarra, L., 2007, Chronostratigraphic framework for the Wilcox Formation (Upper Paleocene–Lower Eocene) in the deep-water Gulf of Mexico: Biostratigraphy, sequences, and depositional systems, *in* L. Kennan, J. Pindall, and N. C. Rosen, eds., The Paleogene of the Gulf of Mexico and Caribbean basins: Processes, events, and petroleum systems: Proceedings of the 27th Annual Gulf Coast Section of the Society of Economic Paleontologists and Mineralogists Foundation Bob F. Perkins Research Conference, p. 81–145.

Zeng, H., Y. He, and L. Zeng, 2021, Impact of sedimentary facies on machine learning of acoustic impedance from seismic data: lessons from a geologically realistic 3D model: Interpretation, v. 9, no. 3, 16 p.

Zeng, H., Y. He, M. I. Olariu, and R. Treviño, 2023, Machine learning-based inversion for acoustic impedance with large synthetic training data: Workflow and data characterization: Geophysics, v. 88, p. R193–R207.

Zhang, J., V. M. Rossi, Y. Peng, R. Steel, and W. Ambrose, 2019, Revisiting late Paleocene Lower Wilcox deltas, Gulf of Mexico: River-dominated or mixed-process deltas?: Sedimentary Geology, v. 389, p. 1–12.

Zhang, J., W. Ambrose, R. Steel, and S. Chen, 2022, Long cores through the Wilcox Group, Gulf of Mexico, show process variability across different time scales: American Association of Petroleum Geologists Bulletin, v. 106, p. 1403–1429.